Neurophysiological evidence of preserved connectivity in tuber tissue

Epilepsy & Behavior Case Reports 7 (2017) 64–68

Contents lists available at ScienceDirect

Epilepsy & Behavior Case Reports

journal homepage: www.elsevier.com/locate/ebcr

Case Report

Neurophysiological evidence of preserved connectivity in tuber tissue

Kaye HL [a,b,c,1], Peters JM [a,c,1], Gersner R [a,b], Chamberland M [d,e], Sansevere A [a], Rotenberg A [a,b,c,*]

[a] Division of Epilepsy and Clinical Neurophysiology, Boston Children's Hospital, Harvard Medical School, Boston, MA, United States
[b] Neuromodulation Program, Boston Children's Hospital, Harvard Medical School, Boston, MA, United States
[c] The F.M. Kirby Neurobiology Center, Boston Children's Hospital, Harvard Medical School, Boston, MA, United States
[d] Computational Radiology Laboratory, Department of Radiology, Boston Children's Hospital, Harvard Medical School, Boston, MA, United States
[e] Sherbrooke Connectivity Imaging Lab, Computer Science Department, Faculty of Science, University of Sherbrooke, Sherbrooke, QC, Canada

ARTICLE INFO

Article history:
Received 17 June 2016
Received in revised form 29 September 2016
Accepted 5 October 2016
Available online 6 October 2016

ABSTRACT

We present a case of preserved corticospinal connectivity in a cortical tuber, in a 10 year-old boy with intractable epilepsy and tuberous sclerosis complex (TSC). The patient had multiple subcortical tubers, one of which was located in the right central sulcus. In preparation for epilepsy surgery, motor mapping, by neuronavigated transcranial magnetic stimulation (nTMS) coupled with surface electromyography (EMG) was performed to locate the primary motor cortical areas. The resulting functional motor map revealed expected corticospinal connectivity in the left precentral gyrus. Surprisingly, robust contralateral deltoid and tibialis anterior motor evoked potentials (MEPs) were also elicited with direct stimulation of the cortical tuber in the right central sulcus. MRI with diffusion tensor imaging (DTI) tractography confirmed corticospinal fibers originating in the tuber. As there are no current reports of preserved connectivity between a cortical tuber and the corticospinal tract, this case serves to highlight the functional interdigitation of tuber and eloquent cortex. Our case also illustrates the widening spectrum of neuropathological abnormality in TSC that is becoming apparent with modern MRI methodology. Finally, our finding underscores the need for further study of preserved function in tuber tissue during presurgical workup in patients with TSC.

1. Introduction

Tuberous sclerosis complex (TSC) is a genetic neurocutaneous syndrome with an estimated incidence of one in 6000–10,000 [1]. TSC is characterized by the development of hamartomas in multiple organs, including the skin, retina, heart, kidney, lung, and in the brain, where they are referred to as tubers. Cortical tubers account for a part of the neuropathological burden in TSC, and contribute to the neurological phenotype of the disease, which includes epilepsy, intellectual disability, and adverse neurodevelopmental and behavioral outcome [2]. At the molecular level, deletion or genetic mutations of the tumor suppressor genes Tsc1 and Tsc2 lead to overactivation of the mechanistic target of rapamycin (mTOR), and to disinhibition of protein synthesis and cell growth. Histopathologically, tubers are collections of abnormally migrated, differentiated and proliferated cells that express a mix of neuronal and glial markers. Abnormalities of cortical lamination, enlarged dysplastic and maloriented neurons, balloon cells positive for both glial and neuronal markers, and extensive astrogliosis are common findings upon analysis of resected tubers [1].

Resective surgery is the only curative option for medically refractory epilepsy in TSC, and >60% of TSC patients with a well localized seizure focus become seizure-free after tuberectomy [3]. Such clinical success motivates exploration into whether and to what extent tubers may have functional connectivity within the brain and spinal cord.

Cortical tubers evident on conventional MRI have long been deemed inert, static lesions that can be safely resected [3]. However, recent neurophysiology, neuropathology, and diffusion imaging demonstrate absence of clear tuber-cortex boundaries, with cortical elements retained within the tuber and extensive tuber-like pathology beyond the tuber [4]. Relevant to the present report, tubers contain maloriented pyramidal cells and dysplastic neurons that suggest a tuber-to-cortex connectivity [5]. Further, tubers, like focal cortical dysplasias, can be in the proximity of eloquent cortex, leading to investigations into whether tubers can contain function [3].

Notably, it is unknown if structural connectivity or neurophysiologic function can be preserved in such imaging-evident lesions, where neuropathology is intermixed with normal cortex.

The lack of clear MRI-defined resection margins, either on tuber interface with cortex or with normal-appearing white matter (NAWM), poses a challenge as long-term success of epilepsy surgery in TSC is directly determined by the total extent of the resection [6]. Further, as more lesions are detected by increasingly high resolution MRI, the

* Corresponding author.
E-mail address: alexander.rotenberg@childrens.harvard.edu (A. Rotenberg).
[1] These authors contributed equally.

http://dx.doi.org/10.1016/j.ebcr.2016.10.001

targeted resection volume may increase, placing eloquent, functional tissue at risk.

To explore potential tuber connectivity with functional brain elements, we employed two modern techniques: Neuronavigated transcranial magnetic stimulation (nTMS), and diffusion tensor imaging.

nTMS is a method for focal noninvasive cortical electrical stimulation where small intracranial electrical currents are generated by a powerful extracranial fluctuating magnetic field. When applied over the motor cortex, nTMS elicits short-latency motor-evoked potentials (MEPs) in a target muscle that reflect connectivity via corticospinal fibers from to the stimulated cortical volume to the anterior horn cell [7]. An FDA-approved nTMS device is used for presurgical mapping of both motor and language cortex. While the current standard of care for preoperative functional localization remains direct current stimulation (DCS) via subdural electrodes, nTMS has been shown to have comparable resolution to that of motor cortex DCS [8]. Moreover, nTMS has a very favorable safety profile and, relevant to our case, is well-tolerated by children with epilepsy. Accordingly, we describe a 10-year old boy with TSC, who underwent nTMS presurgical motor cortex mapping, during which we found evidence of functional connectivity within tuber tissue.

DTI tractography is a technique based on relatively recently developed postprocessing algorithms used to study the 3D configuration of major white matter tracts within cortex tissue. Thus, DTI provides novel insights into the pathological microstructural properties of tuber tissue in patients with TSC [1]. To complement the nTMS findings, DTI tractography was performed.

2. Methods

2.1. Clinical summary

A 10-year-old, left-handed boy with TSC and intractable epilepsy was referred to Boston Children's Hospital Comprehensive Epilepsy Program for consideration of epilepsy surgery.

At birth, he was found to have a cardiac murmur, and echocardiogram showed cardiac rhabdomyomas. A subsequent MRI of the brain revealed classic stigmata of TSC, including subcortical tubers and subependymal nodules. He tested positive for a Tsc2 gene mutation.

Developmentally, the patient's vocabulary was limited to one word by 2 years of age. He began walking at 18 months with difficulties in coordination of complex motor movements. Additionally, the patient struggled with fine motor tasks such as effectively using utensils. At the time of presentation he was able to speak in short sentences and was capable of expressing desire. While the patient was able to use a pencil to scribble on paper, he did not have the capacity to write letters. Neuropsychological testing revealed a 4 year delay behind expected cognitive age. Physical examination was remarkable for hypomelanotic macules on right lower leg, left thigh and left chest, a shagreen patch on the right medial scapula, and facial angiofibromas. On neurological exam he appeared left-handed, but was ambidextrous for some tasks. He had a low central tone but no lateralizing motor findings.

His seizure disorder first presented with infantile spasms, which were successfully controlled with vigabatrin. He then developed focal dyscognitive seizures refractory to multiple anti-epileptic medications, with variable seizure semiology overt time. During evaluation in the epilepsy monitoring unit, seizures began with quivering of the chin, and parent-report stated the patient appeared very frightened. Occasionally bilateral oromotor and hand automatisms were seen during which the patient continued to speak with his mother. EEG revealed interictal discharges in left central and frontocentral areas, and seizures originating in the left central area. 3T MRI with 35 direction DTI revealed subependymal nodules, radial migration lines, and multiple subcortical tubers, in part mineralized, and the largest of which was in the left fronto-parietal area. 2-fluro-deoxy glucose positron-emission tomography (2FDG PET) showed multiple bilateral foci of decreased cortical isotope uptake corresponding to the cortical tubers seen on MRI. Ictal SPECT revealed relative increased perfusion focally in the left frontal lobe when compared to the interictal study. Thus, the active seizure focus was localized to the left frontoparietal tuber complex, and the patient underwent functional mapping to assess the cortical representation of both left and right hemispheric motor control regions.

2.2. nTMS

Verbal and written consent were obtained from the patient's parents prior to stimulation. Electromyography (EMG) was recorded through surface electrodes placed in 6 locations on both the right and left sides of the body over the bilateral abductor pollicis brevis (APB), deltoid, and tibialis anterior (TA) muscle groups. An additional ground electrode was placed on the underside of the right forearm. With single pulse nTMS, stimuli were applied at scalp sites overlying the motor cortex in the right and left hemispheres, while MEPs were recorded bilaterally from the APB, deltoid, and TA by surface EMG.

The patient's MRI DICOM file was uploaded into the Nexstim NBS 4.3 software (Nexstim™, Helsinki, Finland) to create a three-dimensional reconstruction of the patient's cortical surface (Fig. 1). Stimulation was performed with a Nexstim™ unit and a figure-of-eight coil operated with frameless stereotaxy. Motor threshold was operationally defined as the minimum machine output necessary to elicit a response from the APB, contralateral to the stimulated hemisphere, of 50 μV, on >50% of trials.

2.2.1. Data acquisition

The precentral gyrus (M1) and surrounding supplementary motor areas were stimulated to create a map depicting the areas of the cortex

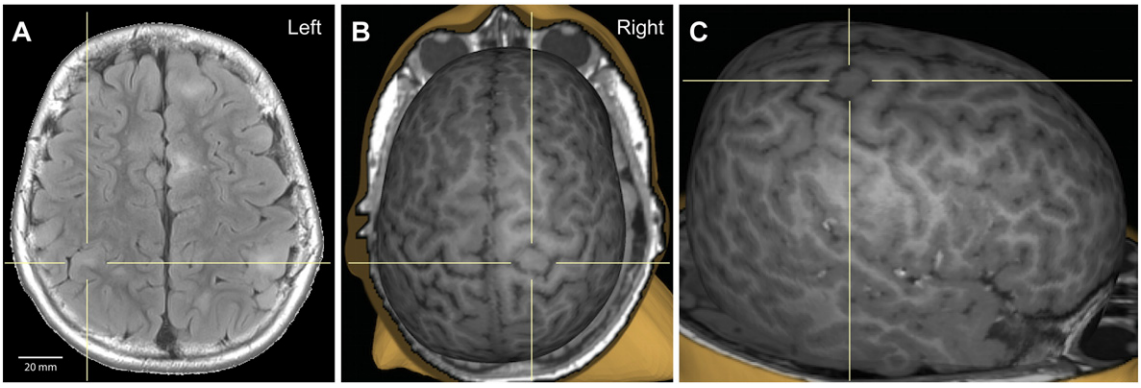

Fig. 1. (A) Axial fluid-attenuated inversion recovery (FLAIR) image, with 20 mm scale-to-size reference. (B and C) 3D MRI reconstruction of the cortical surface with superior (B) and right (C) view. The crosshairs in all panels indicate the cortical tuber.

Table 1
MPRAGE magnetization-prepared rapid acquisition gradient echo; FOV field of view; TE echo time; TR repetition time; FLAIR fluid-attenuated inversion recovery; ETL echo train length; SE spin echo.

	Sequence	Voxel size (mm)	FOV (cm)	TE (ms)	TR (ms)	flip angle	acquisition matrix	other
T1-weighted	MPRAGE	1 × 1 × 1	19.2–25.6	1.66–3.39	1113–2530	7–9		
T2-weighted	Turbo spin echo sequence							
T2-FLAIR	3D isotropic	0.9 × 0.9 × 0.9	19–26	390–400	5000	20	256 × 256	n(excitations) = 1, ETL 141
Diffusion	Single shot SE	1.72 × 1.72 × 1.72	22	88	10	90	128 × 128	30 b = 1000 s/mm2, 5b = 0 s/mm2 images[a]

[a] Twice refocused gradients to minimize Eddy currents, iPAT 2, in-plane GRAPPA, modified as necessary to facilitate completion of the scan.

responsible for eliciting MEPs for a given muscle. The patient had a very high resting APB and deltoid motor threshold (rMT), approximating 100% machine output (MO). Accordingly, upper limb motor mapping was conducted at, 100% MO, as opposed to standard laboratory protocol of stimulating at 120% rMT. TA MEPs could not be elicited at rest, and therefore lower limb motor mapping was conducted with the TA muscles activated by foot dorsiflexion, also at 100% MO – this maneuver was sufficient to enable reliable TA MEPs.

2.2.2. Data processing

Results were reviewed by visual inspection for MEP quality to ensure each individual MEP morphology, latency and distinction form background noise were adequate to designate each signal as a valid motor response to stimulation. To visualize the motor mapping results a voltage-graded color scale was generated per recorded MEP such that lower voltages were shown in red and the highest voltages in white. The color scale was generated separately for each muscle group for minimum and maximum values.

2.3. DTI

Imaging was performed for clinical indication on a Siemens Trio 3T MRI system. Sedation was used to prevent significant motion. MR image analysis was done using the CRKit (http://crl.med.harvard.edu) and visualization was performed using the Fibernavigator [9] (https://github.com/scilus/fibernavigator).

2.3.1. Data acquisition

Imaging acquisition parameters are summarized in Table 1. Compensation for residual distortion and patient motion was achieved by rigid registration of the diffusion images to the T1-weighted MPRAGE scan, with appropriate reorientation of the gradient directions [10]. Tensors were estimated using robust least squares [11].

2.3.2. Data processing

The intracranial cavity was segmented into white matter (WM), gray matter (GM), cortex and cerebrospinal fluid using a previously validated segmentation algorithm, based on the individual T1-weighted image [12–14]. Multi-fiber model estimation was done using DIstribution of Anisotropic MicrOstructural eNvironments in DCI (DIAMOND) [15], resulting in up to 3 main peaks per voxel. With this model, we were able to achieve a sharp representation of the fascicles at each voxel, while maintaining sensitivity to the micro-structural integrity of each fascicle.

2.3.3. Tractography

Whole-brain streamline tractography was performed using real-time multi-peak tractography [9], allowing for interactive visualization of streamlines during the tracking process. Our tractography algorithm employs information from the previous step during tracking, based on an earlier DTI-based approach called tensor deflection [16–18], known to ameliorate neurosurgical tracking [19]. Tractography parameters were set as follows: step size: 1 mm, θ_{max}: 45°, streamline min/max length: 60/200 mm, 1 seed per voxel. WM and GM segmentations were used as tracking masks [20], as they provide an improvement

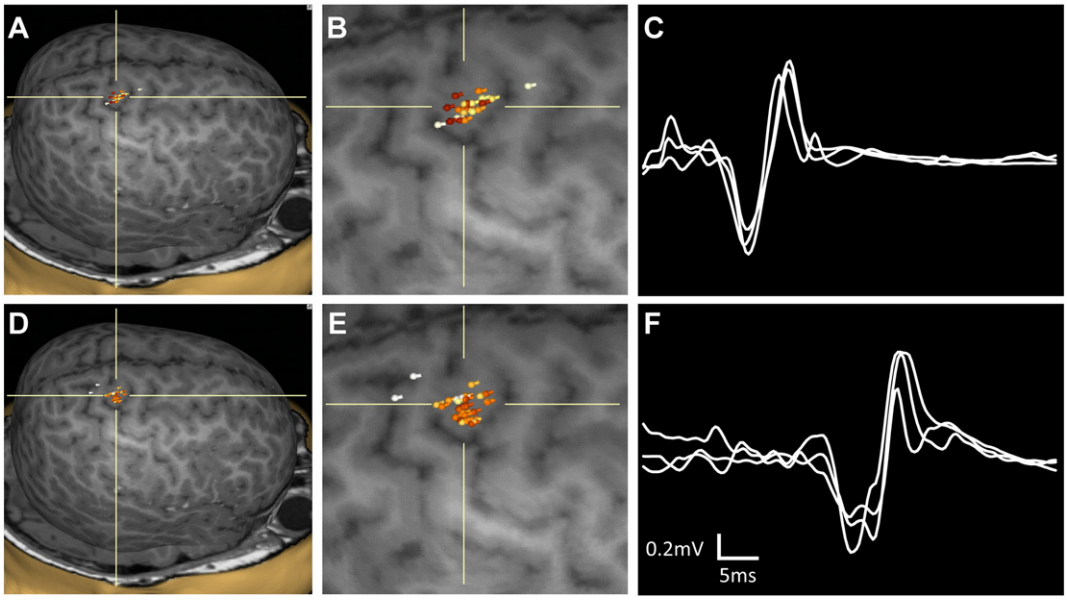

Fig. 2. Composite maps of R hemispheric stimulation sites evoking MEPs of the left deltoid (A) and left tibialis anterior (D) muscles, enlarged in (B) and (E), respectively. The crosshairs indicate the cortical tuber. The 3 highest amplitude MEP traces are overlaid for the left deltoid (C) and left tibialis anterior (F) muscles.

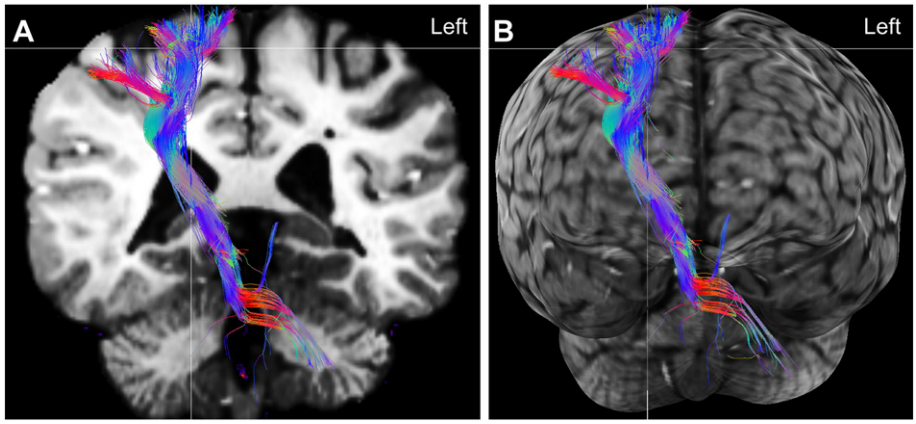

Fig. 3. (A) 3D DTI tractography of the corticospinal tract (colored image) superimposed on a 2D coronal slice of the T1-weighted magnetization-prepared rapid gradient-echo (MPRAGE, black and white image) and (B) the same tractography projected onto a cortical surface rendering, to better depict its trajectory.

compared to fractional anisotropy (FA)-based tracking methods where streamline propagation is often prematurely halted in crossing regions [21–23]. Streamlines were allowed to propagate freely inside the WM, and up to a maximum of 5 consecutive steps once they reached the GM. Finally, 2D streamlines maps were generated using track-density imaging (TDI) [24].

3. Results

3.1. Motor map results

Well-formed right MEPs were elicited with stimulation over M1, as expected, in the left, contralesional hemisphere. However, in the right hemisphere, robust MEPs from the left TA and deltoid were seen with stimulation almost exclusively over a tuber located in the central sulcus, between pre- and postcentral gyrus. Composite maps for our target muscles are shown in Fig. 2. In contrast to the deltoid and TA muscles, the left APB was mapped to the expected hand region of the right precentral gyrus, outside of the tuber tissue.

3.2. DTI results

Streamlines from the DTI tractography of the corticospinal tract (CST) are preserved in the tuber tissue, as shown in Fig. 3. FA values inside the tuber lesion were approximately 0.35, more than sufficient for streamline fascicle propagation using an FA-based approach with a stop criterion. Visual inspection of the diffusion profiles orientation within the tuber showed coherent organization with respect to the peaks forming the CST.

4. Discussion

Our presurgical nTMS motor mapping results indicate that corticospinal (CS) connectivity may be preserved within the volume of some tubers. Specifically, for a cortical tuber located within the central sulcus, (1) MEPs were elicited directly with stimulation of this area, and (2) these MEPs were of similar amplitude and morphology as MEPs elicited in non-tuber cortex. The functional, physiological evidence of connectivity was further corroborated by DTI tractography showing intact CS connectivity within the tuber tissue.

4.1. Neuropathology and function are intermixed in TSC

The success of resective surgery in TSC patients depends upon the accurate identification of the epileptogenic region [6]. Resection of most epileptogenic tubers, perhaps due to a high degree of intra-tuber pathology, appears to be safe with respect to likelihood of acquired neurologic deficit after surgery [3]. Notably, by MRI protocols similar to those in the present report, large tubers appeared to be circumnavigated on DTI tractography [25]. However, our case suggests that CS connectivity may remain intact in some cortical tubers. Further, we show that nTMS in TSC, as in other disorders where functional mapping is required before neurosurgery, can provide insight into local function of targeted tissue, and may also contribute to the prognosis for post-surgical neurologic deficit. (Note that the tuber with preserved CS connectivity was not the surgical target in this case.)

4.2. Incomplete reallocation of function

Early developmental lesions including stroke and malformations of cortical development may allow for transfer of function to adjacent gyri or to more remote regions [8]. Yet, such functional “remapping” was not identified in our case. The lesion burden of the tuber located in the right central sulcus was sufficient to be evident on conventional MRI, but insufficient to disrupt or warrant transfer of motor function. There is no existing literature discussing the possibility of intact motor function within a tuber. Our case begins to address this gap in knowledge. We thus hypothesize that tubers with a relatively small amount of pathology may contain function. The observed physiologic and imaging phenomena, the presence of robust MEPs from nTMS stimulation and preserved CS tracts identified by DTI tractography, within the tuber tissue in our patient provide functional and structural support of the intermixing of tuber and functional tissue. This is in agreement with current pathological [4,26] diffusion imaging [27], and with physiological evidence of widespread and variable degrees of pathology in TSC [28–31].

The color coding of the streamline fascicles represents the main direction of the tract: blue for the super-inferior axis, red for the left-right axis, and green for the anterior-posterior axis. The tuber is located at the crosshair, and is partially obscured by the fiber tract, which travels into the tuber tissue. Note that the fibers do not travel through the ventricles; this is an effect from the superimposition of the 3D tracts onto a 2D coronal plane. The full course of the tract is not all in the same plane as the coronal slice.

Acknowledgments

A. Rotenberg's research is also supported by grants from NIH NINDS (R01NS066019), NIH NIMH (R21MH104318), Boston Children's Hospital Translational Research Program (97631-01), the Smith Family Foundation (94993-01), King Saud University, and the Assimon Family. Dr. Rotenberg is co-founder of and consultant to Neuro'motion Inc., consultant to NeuroRex Inc., and receives or has received in recent past research support from Sage Therapeutics., Wuhan Yirude Medical

Equipment New Technology Co., Ltd., Neuropace, Nexstim, Neuronetics, Brainsway. and Eisai Pharmaceuticals. None of the aforementioned relationships conflict with work described in this manuscript.

H.L. Kaye reports no disclosures or conflicts of interest.

J. Peters is supported by NIH P20 NS080199, R01 NS079788, and U01NS082320 grants and by the Harvard Catalyst|The Harvard Clinical and Translational Science Center (National Center for Research Resources and the National Center for Advancing Translational Sciences, NIH award UL1 TR001102).

R. Gersner reports no disclosures or conflicts of interest.

M. Chamberland's is supported by the Alexander Graham Bell Canada Graduate Scholarships-Doctoral Program (CGS-D3) from the Natural Sciences and Engineering Research Council of Canada (NSERC). None of the aforementioned relationships conflict with work described in this manuscript. A. Sansevere reports no disclosures or conflicts of interest.

References

[1] Peters JM, et al. Diffusion tensor imaging and related techniques in tuberous sclerosis complex: review and future directions. Future Neurol 2013;8(5):583–97.
[2] Spurling Jeste S, et al. Early developmental trajectories associated with ASD in infants with tuberous sclerosis complex. Neurology 2014;83(2):160–8.
[3] Moshel YA, et al. Do tubers contain function? Resection of epileptogenic foci in perirolandic cortex in children with tuberous sclerosis complex. Epilepsia 2010; 51(7):1242–51.
[4] Ruppe V, et al. Developmental brain abnormalities in tuberous sclerosis complex: a comparative tissue analysis of cortical tubers and perituberal cortex. Epilepsia 2014; 55(4):539–50.
[5] Talos DM, et al. Cell-specific alterations of glutamate receptor expression in tuberous sclerosis complex cortical tubers. Ann Neurol 2008;63(4):454–65.
[6] Fallah A, et al. Resective epilepsy surgery for tuberous sclerosis in children: determining predictors of seizure outcomes in a multicenter retrospective cohort study. Neurosurgery 2015;77(4):517–24.
[7] Vitikainen AM, et al. Applicability of nTMS in locating the motor cortical representation areas in patients with epilepsy. Acta Neurochir 2013;155(3):507–18.
[8] Picht T, et al. Preoperative functional mapping for rolandic brain tumor surgery: comparison of navigated transcranial magnetic stimulation to direct cortical stimulation. Neurosurgery 2011;69(3):581–8 [discussion 588].
[9] Chamberland M, et al. 3D interactive tractography-informed resting-state fMRI connectivity. Front Neurosci 2015;9.
[10] Taquet M, et al. A mathematical framework for the registration and analysis of multi-fascicle models for population studies of the brain microstructure. IEEE Trans Med Imaging 2014;33(2):504–17.
[11] Fillard P, et al. Clinical DT-MRI estimation, smoothing, and fiber tracking with log-Euclidean metrics. IEEE Trans Med Imaging 2007;26(11):1472–82.
[12] Grau V, et al. Improved watershed transform for medical image segmentation using prior information. IEEE Trans Med Imaging 2004;23(4):447–58.
[13] Weisenfeld NI, Warfield SK. Automatic segmentation of newborn brain MRI. NeuroImage 2009;47(2):564–72.
[14] Akhondi-Asl A, et al. A logarithmic opinion pool based STAPLE algorithm for the fusion of segmentations with associated reliability weights. IEEE Trans Med Imaging 2014;33(10):1997–2009.
[15] Scherrer B, et al. Characterizing brain tissue by assessment of the distribution of anisotropic microstructural environments in diffusion-compartment imaging (DIAMOND)[Magnetic resonance in medicine] ; 2015.
[16] Lazar M, et al. White matter tractography using diffusion tensor deflection. Hum Brain Mapp 2003;18(4):306–21.
[17] Weinstein, D., G. Kindlmann, and E. Lundberg. Tensorlines: advection-diffusion based propagation through diffusion tensor fields. In Proceedings of the conference on Visualization'99: celebrating ten years. 1999. IEEE Computer Society Press.
[18] Westin C-F, et al. Processing and visualization for diffusion tensor MRI. Med Image Anal 2002;6(2):93–108.
[19] Feigl GC, et al. Magnetic resonance imaging diffusion tensor tractography: evaluation of anatomic accuracy of different fiber tracking software packages. World Neurosurg 2014;81(1):144–50.
[20] Smith RE, et al. Anatomically-constrained tractography: improved diffusion MRI streamlines tractography through effective use of anatomical information. NeuroImage 2012;62(3):1924–38.
[21] Descoteaux, M., High angular resolution diffusion imaging (HARDI). Wiley Encyclopedia of Electrical and Electronics Engineering.
[22] Seunarine KK, Alexander DC. Multiple fibers: beyond the diffusion tensor. Diffusion MRI: from quantitative measurement to in vivo neuroanatomy, 1. ; 2009.
[23] Nimsky C, Bauer M, Carl B. Merits and limits of tractography techniques for the uninitiated, in advances and technical standards in neurosurgery. Springer; 2016 37–60.
[24] Calamante F, et al. Track-density imaging (TDI): super-resolution white matter imaging using whole-brain track-density mapping. NeuroImage 2010;53(4):1233–43.
[25] Peters JM, et al. Loss of white matter microstructural integrity is associated with adverse neurological outcome in tuberous sclerosis complex. Acad Radiol 2012;19(1): 17–25.
[26] Marcotte L, et al. Cytoarchitectural alterations are widespread in cerebral cortex in tuberous sclerosis complex. Acta Neuropathol 2012;123(5):685–93.
[27] Peters JM, et al. Tubers are neither static nor discrete: evidence from serial diffusion tensor imaging. Neurology 2015;85(18):1536–45.
[28] Koh S, et al. Epilepsy surgery in children with tuberous sclerosis complex: presurgical evaluation and outcome. Epilepsia 2000;41(9):1206–13.
[29] Mohamed AR, et al. Intrinsic epileptogenicity of cortical tubers revealed by intracranial EEG monitoring. Neurology 2012;79(23):2249–57.
[30] Major P, et al. Are cortical tubers epileptogenic? Evidence from electrocorticography. Epilepsia 2009;50(1):147–54.
[31] Ma TS, et al. Electrocorticographic evidence of perituberal cortex epileptogenicity in tuberous sclerosis complex. J Neurosurg Pediatr 2012;10(5):376–82.